Journal of Colloid and Interface Science **246,** 372–379 (2002)
doi:10.1006/jcis.2001.8077, available online at http://www.idealibrary.com on IDEAL®

Spreading of Liquid Drops over Saturated Porous Layers

V. M. Starov,*[,1] S. R. Kosvintsev,* V. D. Sobolev,†[,2] M. G. Velarde,‡ and S. A. Zhdanov*

*Department of Chemical Engineering, Loughborough University, Loughborough, Leicestershire, LE11 3TU, United Kingdom; †Moscow Institute of Physical Chemistry, Moscow 117915, Russian Federation; and ‡Instituto Pluridisciplinar, Universidad Complutense, 1 Paseo Juan XXIII, 28040, Madrid, Spain

E-mail: V.M.Starov@lboro.ac.uk; vsobolev@phyche.ac.ru; velarde@fluidos.pluri.ucm.es.

Received June 28, 2001; accepted October 29, 2001; published online January 10, 2002

Spreading of small liquid drops over thin porous layers saturated with the same liquid is investigated from both theoretical and experimental points of view. A theory is presented that shows that spreading is governed by the same power law as in the case of spreading over a dry solid substrate. The Brinkman's equations are used to model the liquid flow inside the porous substrate. An equation of the drop spreading is deduced, which shows that both an effective lubrication and the liquid exchange between the drop and the porous substrates are equally important. The presence of these two phenomena removes the well-known singularity at the moving three-phase contact line. Matching of the drop profile in the vicinity of the three-phase contact line with the main spherical part of the drop gives the possibility to calculate the pre-exponential factor in the spreading law via permeability and effective viscosity of the liquid in the porous layer. Unfortunately, the latter dependency turns out to be very weak. Spreading of silicone oils over different microfiltration membranes is carried out. Radii of spreading on time experimental dependencies confirm the theory predictions. Experimentally found coefficients agree with theoretical estimations.

Key Words: **porous layer; capillary spreading.**

INTRODUCTION

Spreading of liquids over solid surfaces is a fundamental process with a number of applications such as coating, printing, and painting. For the most part the spreading over smooth homogeneous surfaces has been considered (1–5). It has been established that singularity at the three-phase contact line is removed by the action of surface forces (4, 5). However, the vast majority of real solid surfaces are rough to a different degree and in many cases surfaces are either porous or covered with a thin porous sublayer. The presence of roughness and/or a porous sublayer obviously changes the spreading conditions (6–8). Theoretical descriptions of the spreading over real surfaces is usually based on an empirical "slippage condition" introduced in (9). In spite of the progress achieved based on the utilization of this condition (10–13), the question remains if the "slippage condition" has any theoretical background. The Brinkman's equations (14), though not completely rigorously deduced (15), have at least a reasonable semi-empirical background with physically meaningful coefficients: an effective viscosity and a permeability coefficient. A new way of calculation of these coefficients as functions of the porosity of the porous media has been suggested (16).

An attempt to use the Brinkman's equations for description of the flow inside the porous layer coupled with the drop flow over the layer has been undertaken in (17). Below, the same approach is applied to the investigation of the spreading of liquid drops over thin porous substrates filled with the same liquid. The Brinkman's equations are used for description of the liquid flow inside the porous substrate. The thickness of the porous substrate, Δ, is assumed much smaller than the drop height, H^*.

THEORY

Kinetics of spreading of small liquid drops over thin porous layers saturated with the same liquid is investigated below. Theoretical consideration takes into account kinetics of liquid motion both in the drop above the porous layer and inside the porous layer itself. Consideration of the flow inside the porous layer is based on Brinkman's equations.

Liquid inside the drop ($0 < z < h(t, r)$*, Fig. 1).* Let us consider the spreading of an axisymmetric liquid drop over a thin porous layer with thickness Δ saturated with the same liquid. The thickness of the porous layer is assumed much smaller than the drop height, that is, $\Delta \ll H^*$, where H^* is the scale of the drop height. The drop profile is assumed having a low slop ($H^*/L^* \ll 1$, where L^* is the length scale of the drop base). The influence of the gravity is neglected (small drops, bond number $\ll 1$). That is, only capillary forces are taken into account below.

In the case under consideration the liquid motion inside the drop is described by the following system of equations,

$$\frac{\partial p}{\partial r} = \mu \frac{\partial^2 v}{\partial^2 z^2} \qquad [1]$$

[1] To whom correspondence should be addressed.

[2] Current position: Visiting Professor, Department of Chemical Engineering, Loughborough University, Loughborough, Leicestershire, LE11 3TU, U.K. E-mail: v.sobolev@lboro.ac.uk.

0021-9797/02 $35.00

$$\frac{\partial p}{\partial z} = 0 \qquad [2]$$

$$\frac{1}{r}\frac{\partial (rv)}{\partial r} + \frac{\partial u}{\partial z} = 0, \qquad [3]$$

and boundary conditions,

$$v = v^0, \quad u = u^0, \quad z = +0 \qquad [4]$$

$$\frac{\partial v}{\partial z} = 0, \quad z = h(t, r) \qquad [5]$$

$$p = p_g - \frac{\gamma}{r}\frac{\partial}{\partial r}\left(r\frac{\partial h}{\partial r}\right), \qquad [6]$$

where t is the time, r and z are radial and vertical coordinates, respectively, $z > 0$ and $-\Delta < z < 0$ correspond to the drop and the porous layer, respectively, $z = 0$ is the drop–porous layer interface, p, v, and u are the pressure, radial, and vertical velocity components, respectively, v^0 and u^0 are velocity components at the drop–porous layer interface, which are determined below by coupling with the flow inside the porous layer, $h(t, r)$ is the drop profile, γ is the liquid–air interfacial tension, and p_g is the pressure in ambient air.

Equations [1] and [2] are Stokes equations, in the low slope case; Eq. [3] is the incompressibility condition; Eq. [5] shows an absence of a tangential stress on the liquid–air interface; Eq. [6] presents the pressure jump on the same interface.

Integration of Eqs. [1]–[3] with boundary conditions [4]–[6] results in the following equation, which describes the evolution of the drop profile:

$$\frac{\partial h}{\partial t} = u^0 - \frac{1}{r}\frac{\partial}{\partial r}\left\{r\left[h^3\frac{\gamma}{3\mu}\frac{\partial}{\partial r}\left(\frac{1}{r}\frac{\partial}{\partial r}\left(r\frac{\partial h}{\partial r}\right) + v^0 h\right)\right]\right\}. \qquad [7]$$

The liquid velocity components, v^0 and u^0, on the drop–porous layer interface are calculated below.

Inside the porous layer beneath the drop ($-\Delta < z < 0, 0 < r < L$, Fig. 1). If the porous layer is not completely saturated, then the capillary pressure inside the saturated part of the porous layer, p_c, can be estimated as

$$p_c \approx \frac{\gamma}{a^*},$$

where a^* is the scale of capillary radius inside the porous layer. According to Eq. [6], the capillary pressure inside the drop, $p - p_g$, can be estimated as

$$p_g - p \approx \frac{\gamma h^*}{L^{*2}} = \frac{h^*}{L^*}\frac{\gamma}{L^*} \ll \frac{\gamma}{L^*} \ll \frac{\gamma}{a^*} \approx p_c.$$

That is, the capillary pressure inside the spreading drop is many orders of magnitude smaller than the capillary pressure inside the porous layer in the case of noncomplete saturation. The latter means that the drop pressure cannot disturb in any way the drop–porous layer interface in front of the spreading drop when the porous layer is completely saturated. Hence, this interface always coincides with the surface $z = 0$. It is worth mentioning that everything is going on time scales much bigger than the initial period considered in (18).

The liquid motion inside the porous layer with thickness Δ is assumed to obey Brinkman's equations. In this case the liquid motion inside the porous layer is described by the following system of equations,

$$\frac{\partial p}{\partial r} = \mu_p\frac{\partial^2 v}{\partial^2 z^2} - \frac{v}{K_p} \qquad [8]$$

$$\frac{\partial p}{\partial z} = 0 \qquad [9]$$

$$\frac{1}{r}\frac{\partial (rv)}{\partial r} + \frac{\partial u}{\partial z} = 0, \qquad [10]$$

and boundary conditions,

$$v = v^0, \quad u = u^0, \quad z = -0 \qquad [11]$$

$$\frac{\partial v}{\partial z} = u = 0, \quad z = -\Delta \qquad [12]$$

$$\mu_p\frac{\partial v}{\partial z}\bigg|_{z=-0} = \mu\frac{\partial v}{\partial z}\bigg|_{z=+0}, \qquad [13]$$

$$p|_{z=-0} = p|_{z=+0}, \qquad [14]$$

where μ_p and K_p are the viscosity and permeability of the Brinkman's medium, respectively. The first of boundary condition [12] corresponds to the absence of a tangential stress on the lower boundary of the porous layer, which corresponds to experimental conditions (see below).

Let us introduce Brinkman's radius as

$$\delta = \sqrt{\mu_p K_p}. \qquad [15]$$

Solution of Eqs. [8]–[10] with boundary conditions [11]–[15] gives

$$v^0 = -\frac{1}{\mu_p}\left(h\delta\,\coth\frac{\Delta}{\delta} + \delta^2\right)\frac{\partial p}{\partial r},$$

$$u^0 = \frac{2}{\mu_p}\frac{1}{r}\frac{\partial}{\partial r}\left[r(h\delta^2 + \Delta\delta^2)\frac{\partial p}{\partial r}\right]. \qquad [16]$$

Substitution of the latter expressions into Eq. [7] results in the following equation, which describes the kinetics of spreading of a liquid drop over a porous substrate,

$$\frac{\partial h}{\partial t} = -\frac{\gamma}{3\mu}\frac{1}{r}\frac{\partial}{\partial r}\left\{r\left(h^3 + 3\alpha\,\coth\frac{\Delta}{\delta}h^2\delta + 6\alpha h\delta^2 + 3\alpha\delta^2\Delta\right)\right.$$
$$\left.\times\frac{\partial}{\partial r}\left(\frac{1}{r}\frac{\partial}{\partial r}\left(r\frac{\partial h}{\partial r}\right)\right)\right\}, \qquad [17]$$

where $\alpha = \mu/\mu_p$ is the viscosity ratio. According to (16), effective viscosity, μ_p, is always higher than the liquid viscosity, μ; that is, $\alpha < 1$.

If instead of Brinkman's equation [8] a slip condition on the liquid–porous layer interface is used (11), then the vertical velocity component, u^0, should be set to zero in Eq. [7] and the following boundary condition should be adopted for the radial velocity component,

$$\left.\frac{\partial v}{\partial z}\right|_{z=0} = \frac{\beta}{\delta}(v^0 - v_p), \qquad [18]$$

where β is an empirical parameter and

$$v_p = -\frac{K_p}{\mu_p}\frac{\partial p}{\partial r}$$

is the velocity inside the porous substrate; δ/β is a slip length.

If boundary conditions [13] and [18] are compared, then it is easy to see that the latter one can be directly obtained from condition [18] if we adopt

$$\mu_p \left.\frac{\partial v}{\partial z}\right|_{z=-0} = \mu_p \frac{v^0 - v_p}{\delta}.$$

A combination of the latter expression and boundary condition [13] gives the following value of empirical coefficient β:

$$\beta = \frac{1}{\alpha}. \qquad [19]$$

The latter means that the slip length is equal to

$$\alpha\delta = \mu\sqrt{\frac{K_p}{\mu_p}}.$$

K_p and μ_p dependencies on porosity can be calculated according to (16).

However, the omitted contribution of a vertical component, u^0, gives the comparable contribution in the resulting equation (see below).

Equation [17] should be solved with the symmetry condition in the drop center:

$$\frac{\partial h}{\partial r} = \frac{\partial^3 h}{\partial r^3} = 0, \quad r = 0, \qquad [20]$$

and conservation of the drop volume condition,

$$2\pi \int_0^L r h\, dr = V, \qquad [21]$$

where $L(t)$ is the macroscopic radius of the drop base (Fig. 1).

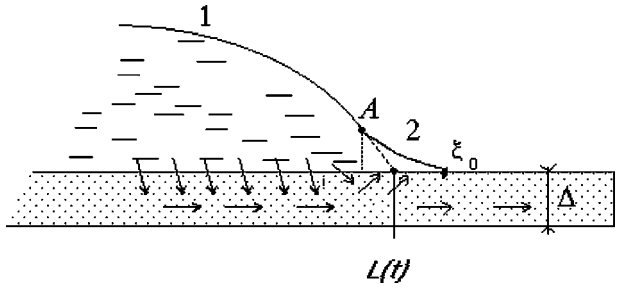

FIG. 1. Spreading of a liquid drop over a saturated porous layer of thickness Δ. 1, outer region (spherical cap); 2, inner region. Inflections point A separates the inner and outer regions. Inside the outer region liquid flows from the drop into the porous layer; inside the inner region the liquid flows from the porous layer into the drop edge. $L(t)$, macroscopic radius of the drop base.

Everywhere at $r < L(t)$ except for a narrow region, ξ, close to the three-phase contact line, the following inequality holds: $h \gg \delta$. The size of this narrow region close to the three-phase contact line is calculated below. The same consideration as in (5) shows that solution of Eq. [17] can be presented as "outer" and "inner" solutions (Fig. 1). The "outer" solution can be deduced in the following way: the left-hand side of Eq. [17] should be set to zero and solved with boundary conditions [20], [21], and

$$h(t, L - \xi) \approx 0. \qquad [22]$$

This procedure gives in the same way as in (5) the "outer" solution in the following form:

$$h(t, r) = \frac{2V}{\pi L^4}(L^2 - r^2), \quad r < L(t) - \xi. \qquad [23]$$

Equation [23] shows that the drop profile retains the spherical shape over the duration of spreading (except for a very short initial stage).

The drop slope at the macroscopic edge can be found from [23] as

$$\left.\frac{\partial h}{\partial r}\right|_{r=L} = -\frac{4V}{\pi L^3}, \qquad [24]$$

which is used below as a boundary condition for the "inner" solution.

Inside the inner region (Fig. 1) the solution can be represented in the following form,

$$h(t, r) = \delta f(\zeta), \quad \zeta = \frac{r - L(t)}{\chi(t)}, \qquad [25]$$

where f is a new unknown function, ζ is a similarity variable, and $\chi(t) \ll L(t)$ is the scale of the "inner" region. This means that $\xi \approx \chi(t)$. Substitution of the solution in the form [25] into

Eq. [17] results in the following equation for $f(\zeta)$ determination,

$$\frac{df}{d\zeta}\dot{L}(t) = \frac{\gamma}{3\mu}\frac{\delta^3}{\chi^3(t)}\frac{d}{d\zeta} \times \left[\left(f^3 + 3\alpha\ \coth\frac{\Delta}{\delta}f^2 + 6\alpha f + 3\alpha\frac{\Delta}{\delta}\right)\frac{d^3 f}{d\zeta^3}\right], \quad [26]$$

where the overhead dot means the differentiation with respect to t and small terms are neglected in the same way as in (5).

The latter equation should not depend on time; this gives two equations:

$$\dot{L}(t) = \frac{\gamma}{3\mu}\frac{\delta^3}{\chi^3(t)} \quad [27]$$

and

$$\frac{df}{d\zeta} = \frac{d}{d\zeta}\left[\left(f^3 + 3\alpha\ \coth\frac{\Delta}{\delta}f^2 + 6\alpha f + 3\alpha\frac{\Delta}{\delta}\right)\frac{d^3 f}{d\zeta^3}\right]. \quad [28]$$

The solution of Eq. [28] should be matched with outer solution [23]. Matching of asymptotic solutions gives the following condition:

$$\frac{\delta}{\chi(t)}\frac{df}{d\zeta}\bigg|_{\zeta\to\infty} = \frac{4V}{\pi L^3(t)}. \quad [29]$$

The latter condition should not depend on time t, which gives

$$\frac{df}{d\zeta}\bigg|_{\zeta\to-\infty} = \lambda \quad [30]$$

and

$$\lambda = \frac{4V\chi(t)}{\pi L^3(t)\delta}, \quad [31]$$

where λ is a dimensionless constant (see below). The latter equation gives

$$\chi(t) = \delta\frac{\pi L^3(t)\lambda}{4V} \ll L(t). \quad [32]$$

This means that the scale of the inner region (Fig. 1) is proportional to δ and is actually very small as compared with the drop base.

A combination of Eqs. [31] and [27] gives the following equation for the radius of spreading, $L(t)$, determination:

$$L^9(t)\dot{L}(t) = \frac{\gamma}{3\mu}\left(\frac{4V}{\pi\lambda}\right)^3. \quad [33]$$

The solution of the latter equation with initial condition $L(0) = L_0$, where L_0 is the initial drop radius, is

$$L(t) = L_0\left(1 + \frac{t}{\tau}\right)^{0.1}, \quad [34]$$

where $\tau = \frac{3\mu L_0}{10\gamma}(\frac{\pi\lambda L_0^3}{4V})^3$ is the time scale of the spreading process.

Now back to the parameter λ determination. Integration once of Eq. [28] and setting an integration constant zero (because of conservation of the drop volume and vanishing of the drop profile in front of the spreading drop) gives

$$\frac{d^3 f}{d\zeta^3} = \frac{f}{f^3 + 3\alpha\ \coth\frac{\Delta}{\delta}f^2 + 6\alpha f + 3\alpha\frac{\Delta}{\delta}}. \quad [35]$$

This equation should be solved with the following boundary conditions,

$$f(\varsigma_0) = \frac{df(\varsigma_0)}{d\zeta} = 0, \quad [36]$$

and boundary condition [30]. Unfortunately, it is well known that the latter condition cannot be satisfied because Eq. [35] does not have a proper asymptotic behavior (5, 21). An approximate method ("patching" of asymptotic solutions) has been suggested in (5, 21), which allows an approximate determination of parameter λ. Now, the unknown constant λ can be calculated in the same approximate way as has been done in (5, 21). However, estimations below show, however, that it is not worth doing this.

The second of two boundary conditions [36] means a zero microcontact angle on the microscopic drop boundary.

Equation [24] gives the following value of an apparent dynamic contact angle, θ, $(\tan\theta \approx \theta)$:

$$\theta = \frac{4V}{\pi L^3}, \quad [37]$$

or

$$L = \left(\frac{4V}{\pi\theta}\right)^{1/3}. \quad [38]$$

A combination of Eqs. [38] and [33] results in

$$\frac{dL}{dt} = \omega\frac{\gamma\theta^3}{\mu}, \quad [39]$$

where $\omega = 1/3\lambda^3$ is referred to below as an "effective lubrication coefficient". If liquid spreads over a solid substrate, an "effective lubrication" is determined by the surface forces action in the vicinity of the three-phase contact line (5). In this case the "effective lubrication coefficient" has been calculated (5) and its value is 1.36×10^{-2}. It is reasonable to expect an ω value higher than the latter one in the case under consideration. Spreading

TABLE 1

Membrane pore size	L_0 (cm)	μ (P)	τ (s)	V (cm^3)	ω
0.2 μm	0.176	5.58	0.333	0.0039	0.017 ± 0.004
0.2 μm	0.193	0.558	0.0592	0.0040	0.018 ± 0.004
0.2 μm	0.150	1.18	0.00163	0.003	0.014 ± 0.005
0.2 μm	0.150	1.18	0.0026	0.0034	0.014 ± 0.003
0.2 μm	0.165	1.18	0.0086	0.003	0.016 ± 0.005
3 μm	0.119	1.18	0.0546	0.0055	0.015 ± 0.009
3 μm	0.250	1.18	0.461	0.005	0.016 ± 0.009
3 μm	0.253	0.558	0.609	0.005	0.018 ± 0.08
Optical glass	0.226	0.558	0.0378	0.0068	0.012 ± 0.03
Optical glass	0.113	1.18	0.0103	0.002	0.010 ± 0.05

of liquid over a prewetted solid substrate has been considered in (21). An effective lubrication coefficient in this case has been calculated as 1.6×10^{-2}. The latter shows

(a) The effective lubrication coefficient is not very sensitive to experimental conditions. That is, we have chosen not to try to calculate it theoretically though the procedure of its approximate determination is very similar to those presented in (5) or (21).

(b) It is reasonable to expect values of the effective lubrication coefficient in between these two values. Experimentally found values of the effective lubrication coefficient agree with our estimations reasonably well (see Table 1).

MATERIALS AND METHODS

Silicone oils SO50 (viscosity 0.554 P), SO100 (viscosity 1.18 P), and SO500 (viscosity 5.582 P) purchased from "PROLABO" are used in our spreading experiments. Cellulose nitrate membrane filters purchased from Sartorius (type 113) with an averaged pore size 0.2 and 3 μm, respectively, are used as porous layers. All membranes samples used are a circle plane plate with the radius 25 mm and thickness from 0.0130 to 0.0138 cm. The porosity of membranes ranges between 0.65 and 0.87.

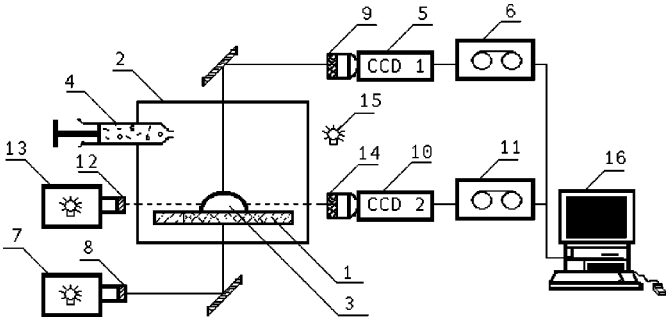

FIG. 2. Experimental setup. 1, wafer; 2, sample chamber; 3, tested drop; 4, dosator; 5 and 10, CCD cameras; 6 and 11, VCRs; 7 and 13, illuminators, 8, 9, 12 and 14, interferential light filters (8 and 9 with wavelength 520 nm and 12 and 14 with wavelength 640 nm).

Prior to spreading experiments, membranes were dried for 3–5 h at 95°C and then stored in a dry atmosphere.

Figure 2 shows the sample chamber for monitoring the drop spreading over porous layers and dynamic contact angles. A porous wafer, 1 (Fig. 2), is placed in a thermostated and hermetically closed chamber, 2, with a fixed humidity and temperature. The chamber was made of brass to prevent temperature and humidity fluctuations. In the chamber walls several channels were drilled, which are used for pumping a thermostating liquid. The chamber is equipped with a fan. The temperature is monitored by a thermocouple. Droplets of liquid, 3, are placed onto a wafer by a dosator, 4 (Fig. 2). The volume of drops is set by the diameter of the separable capillary of the dosator.

The chamber is also equipped with optical glass windows for observation of both the spreading drop shape and size (side view and view from above). Two CCD cameras and two tape recorders are used for storing of the sequences of spreading. Different colors of monochromatic light are used for a side view and view from above to eliminate spurious illumination on images. The optical circuit for viewing from above (illuminator, 7, as well as the camera, 5) are equipped with interferential light filters, 8 and 9, with wavelength 520 nm. The side view curcuit (the illuminator, 13, and camera, 10) are equipped with filters, 12 and 14, with wavelength 640 nm. Such arrangement suppresses the illumination of a CCD camera, 2, by the diffused light from the membrane and, hence, increases the precision of measurements. The automatic processing of images is carried out using the image processor "Scion Image". The time discretization in processing ranges from 0.1 to 1 s in different experiments; the size of a pixel on the image corresponds to 0.0125 mm.

The experiments are organized in the following order:

—A membrane under investigation is placed in the chamber.

—A big drop of oil is deposited. The volume of the drop, V, is selected as $V = \pi m \Delta R_m^2$, where R_m is the radius of the membrane sample. This choice corresponds to the complete saturation of the membrane by a tested liquid.

—After the imbibition process is completed (100–500 s depending on the liquid viscosity), the next tiny drop of the same liquid is deposited on the saturated porous layer and the spreading of this drop is monitored. Volumes of drops are measured by the direct evaluation of video images. Precision of measurement is around 0.0001–0.0005 cm^3.

RESULTS AND DISCUSSION

Experimental Determination of "Effective Lubrication Coefficient" ω

According to our observations in all spreading experiments, drops retain the spherical shape and no disturbances or instabilities are detected. Experimental data are fitted using the following dependency:

$$L = L_0(1 + t/\tau)^n. \qquad [40]$$

It is necessary to comment on the adopted fitting procedure.

If experimentally determined values of the exponent, n, are taken from review (19), it is easy to see that in most cases this exponent is higher (sometimes considerably) than 0.1. Below, we present a possible explanation of this phenomenon, which we encountered in our experiments.

In all our experiments (as probably in a number of others too) drops have been placed on the solid substrate using a syringe. That is, actually, drops fall from some height. The latter means that during the very short the initial stage of spreading both inertia and a relaxation of the drop shape could not be ignored. That means, during the initial stage of spreading both the Reynolds number, *Re*, and the capillary number, *Ca*, are not small and the capillary regime of spreading is not applicable during this initial stage of spreading. Inertia spreading has been considered in (20), where the following spreading law has been predicted:

$$L(t) = v_\infty t, \qquad [41]$$

where

$$v_\infty = \left(\frac{24\gamma}{\rho L_0}\right)^{1/2}$$

and ρ is the liquid density. The latter equation shows that during the inertia spreading regime the drop spreads much faster than during the capillary regime of spreading. Derivation in (20) is applicable only if the Reynolds number is high enough. Let us estimate the Reynolds number, which is

$$Re = \frac{v_\infty H(t)\rho}{\mu},$$

where $H(t)$ is the maximum drop height. According to (20),

$$H(t) = \frac{V}{L^2(t)}$$

during the inertia period of spreading. Condition $Re \gg 1$ gives

$$\frac{V\rho}{\mu}\left(\frac{\rho L_0}{24\gamma}\right)^{1/2}\frac{1}{t^2} \gg 1 \quad \text{or}$$

$$t \ll t_{Re}, \quad t_{Re} = \left(\frac{V\rho}{\mu}\right)^{1/2}\left(\frac{\rho L_0}{24\gamma}\right)^{1/4}. \qquad [42]$$

t_{Re} values relevant to our experiments are calculated below. Let us estimate the Reynolds number during the capillary spreading stage. Equation [39] gives the velocity of spreading, which should be used for calculation of the Reynolds number. Simple rearrangement gives

$$Re = \frac{\omega\gamma\theta^3 L}{\mu^2} \approx 10^{-2}.$$

The latter estimation should be compared with Eq. [42], which gives

$$\left(\frac{t_{Re}}{t}\right)^2 \approx 10^{-2} \quad \text{or} \quad t \sim 10t_{Re} \sim 0.1 \text{ s}.$$

This means that the capillary regime of spreading takes place only at $t > 10t_{Re}$.

Equation [39] is used below to determine the condition for the fulfillment of the second requirement, $Ca \ll 1$. The latter equation can be rewritten as $Ca = \omega\theta^3$. According to our experimental condition $\omega \approx 10^{-2}$, $\theta \approx 0.5$. This gives the following estimation of the capillary number: $Ca \sim 10^{-3}$. The latter means

$$\frac{U\mu}{\gamma} \approx \frac{L\mu}{t\gamma} \approx 10^{-3} \quad \text{or} \quad t \sim 10^3 \quad t_{Ca} \sim 1 \text{ s},$$

where

$$t_{Ca} = \frac{L\mu}{\gamma}.$$

It is necessary to emphasize that t_{Re} is reversibly proportional to $\mu^{1/2}$ (that is, decreases with the viscosity increase) but t_{Ca} is proportional to the viscosity (that is, increases with viscosity increase). This corresponds well to our experimental observations.

In any experimental observation only a limited number of experimental values of $L(t)$ dependency is measured. If some of these measurements are taken at the initial regime of spreading, then it results in a higher value of the fitted exponent than 0.1.

For example, let us take the experimental curve in the case of spreading of SO50 over a saturated porous layer (Figs. 3a and 3b). In Fig. 3a this dependency is presented in a log–log coordinate system. It is easy to see that the whole spreading process consists of two stages corresponding to two different power laws. During the first stage inertia/shape relaxation can not be neglected while on the second stage capillary spreading (exponent close to 0.1) takes place. In Fig. 3b the fitting results for this particular spreading experiment are presented. The broken line corresponds to the fitting procedure when all experimental points are taken into account. In this case the fitted exponent is higher than 0.1 (0.13 ± 0.01). However, if we do not take into account the first three points, located within the initial stage of spreading, then the fitted exponent becomes 0.11 ± 0.01, that is, much closer to 0.1. Figure 3a shows that the initial stage of spreading continues approximately around 0.1 s, which agrees reasonably well with the above estimations.

The following procedure for the definition of the parameters L_0 and τ is adopted. First, the points which correspond to

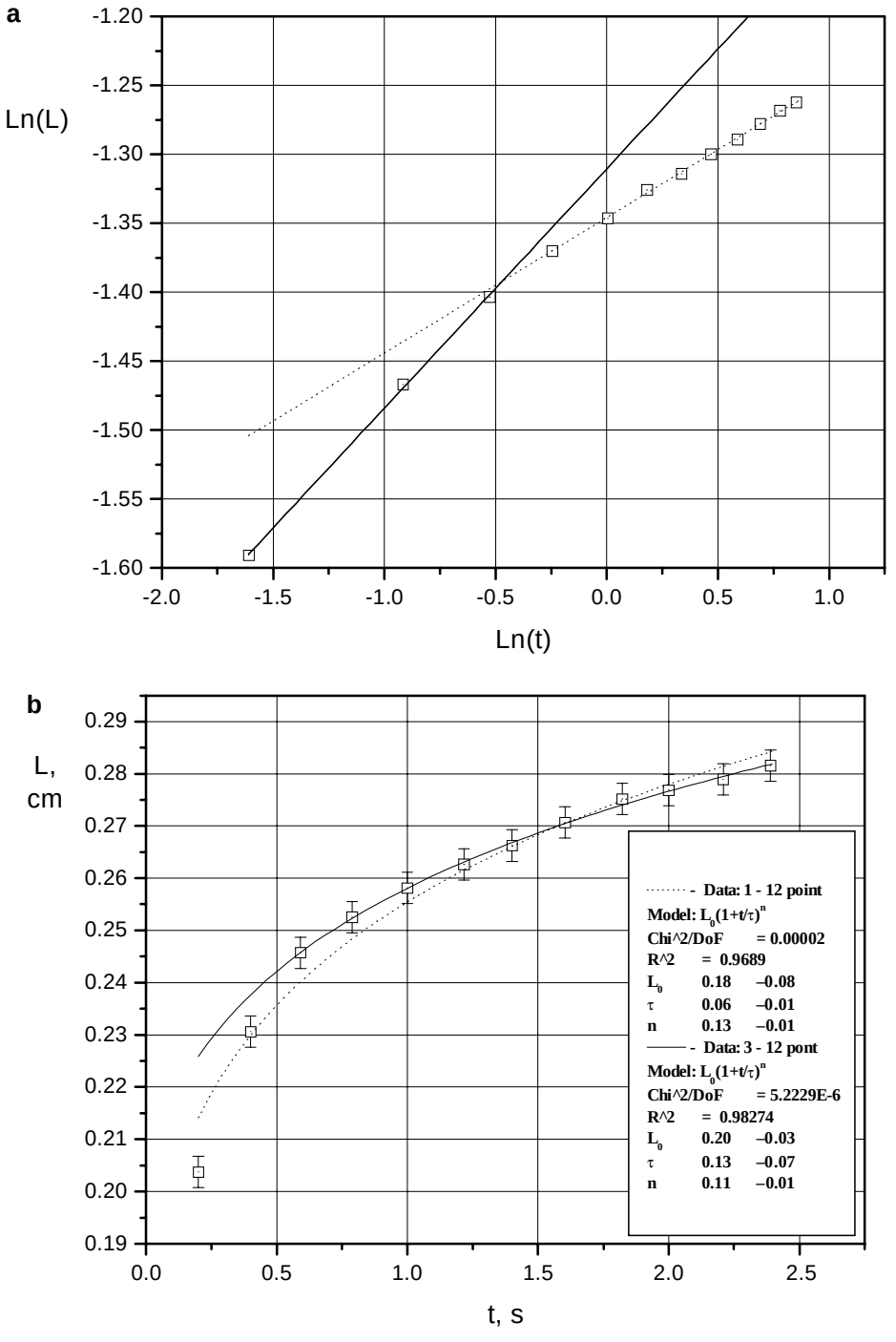

FIG. 3. (a) Radius of the drop base on time in log–log coordinates. SO50 drop, volume 0.0039 cm^3, membrane with average pore size 0.2 μm. (b) Radius of the drop base on time. SO50 drop, volume 0.0039 cm^3, membrane with average pore size 0.2 μm. Broken line, fitted using all experimental poins; solid line, fitted using only points that correspond to the capillary stage of spreading. Fitted parameters are given in the insert.

the capillary stage of spreading are selected using the presentation of experimental points in a log–log coordinate system. After this the fitting procedure using Eq. [40] is carried out using only experimental points, which correspond to the capillary stage of spreading. This procedure gives values of L_0 and τ in each run.

After experimental definition of L_0 and τ the value of ω is calculated in the following way. Equation [34] can be rewritten as

$$L = L_0\left(1 + 10\left(\frac{4}{\pi}\right)^3 \frac{V^3\gamma}{L_0^{10}\mu}\omega\, t\right)^{0.1}. \qquad [43]$$

A comparison of Eqs. [43] and [40] gives

$$\omega = \left(\frac{\pi}{4}\right)^3 \frac{1}{\tau} \frac{L_0^{10}}{V^3} \frac{\mu}{10\gamma}. \qquad [44]$$

Determined values of ω as well as other experimental parameters are presented in Table 1. For comprising in the same Table 1 the results of the spreading over a dry glass (microscope optical glass) are presented (last two rows). The data presented in Table 1 show that (i) the effective lubrication coefficient is higher in the case of spreading over a saturated porous substrate than in the case of "dry spreading" and (ii) experimentally determined values of the effective lubrication coefficient, ω, agree well with the above theoretical estimations. However, precision of experimental determination of this parameter does not allow us to extract more information about the effective viscosity of the porous substrate.

ACKNOWLEDGMENTS

This research is sponsored by Grant GR/R 07578 from the U.K. Engineering and Physical Sciences Research Council and by Grant PB 96-599 from the Spanish Ministerio de Ciencia y Tecnologia.

REFERENCES

1. Starov, V. M., *Colloid J.* (USSR Academy of Sciences, English Translation) **45**(6), 1154 (1983).
2. De Gennes, P. G., *Rev. Mod. Phys.* **57,** 827 (1985).
3. Joanny, J.-F., *J. Mecanique Theor. Appl.* **5,** 249 (1986).
4. Teletzke, G. F., Davis, T. H., and Scriven, L. E., *Chem. Eng. Commun.* **55,** 41 (1987).
5. Starov, V. M., Kalinin, V. V., and Chen, J.-D., *Adv. Colloid Interface Sci.* **50,** 187 (1994).
6. Raphael, E., and de Gennes, P. G., *C. R. Acad. Sci. Paris* **327,** Ser. IIb, 685 (1999).
7. Bacri, L., and Brochard, F., *Eur. Phys. J. E* **3,** 87 (2000).
8. Aradian, A., Raphael, E., and de Gennes, P. G., *Eur. Phys. J. E* **2,** 367 (2000).
9. Beaverse, G., and Johns, D., *J. Fluid Mech.* **30**(1), 197 (1967).
10. Greenspan, H. P., *J. Fluid Mech.* **84,** 125 (1978).
11. Neogi, P., and Miller, C. A., *J. Colloid Interface Sci.* **92**(2), 338 (1983).
12. Davis, S. H., and Hocking, L. M., *Phys. Fluids* **11**(1), 48 (1999).
13. Davis, S. H., and Hocking, L. M., *Phys. Fluids* **12**(7), 1646 (2000).
14. Brinkman, H., *J. Chem. Phys.* **20,** 571 (1952). Brinkman, H., *Appl. Sci. Res. A* **1,** 27 (1947).
15. Whitaker, S., "The method of volume averaging," Kluwer, Dortrecht, 1999.
16. Starov, V. M., and Zhdanov, V. G., *Colloids Surf. A* **192,** 363 (2001).
17. Kalinin, V. V., and Starov, V. M., *Colloid J.* (USSR Academy of Sciences, English Translation) **51**(5), 860 (1989).
18. Kornev, K. G., and Neimark, A. V., *J. Colloid Interface Sci.* **235,** 101 (2001).
19. Marmur, A., *Adv. Colloid Interface Sci.* **19,** 75 (1983).
20. Joanny, J.-F., *J. Phys.* **46,** 807 (1985).
21. Kalinin, V., and Starov, V. *Colloid J.* (USSR Academy of Sciences, English Translation) **48**(5), 767 (1986).